PHILIPPINE ENGINEERING JOURNAL
PEJ 2026; Vol. 47, No. 1:34-56

Received: 13 January 2026
Received in Revised Form: 27 April 2026
Accepted: 26 May 2026

Wave Energy Resource Assessment Off the Coast of Miliga-biga Beach, Bulusan, Sorsogon by Prevailing Wave Modelling

Dominic M. Bautista*, Cesar M. Gapas Jr., Marjorie T. David
Institute of Civil Engineering, College of Engineering
University of the Philippines Diliman, Quezon City, Metro Manila, Philippines
**Corresponding author: dmbautista2@up.edu.ph*

Abstract *– In the Philippines' pursuit to shift to renewable energy, locations such as off the coast of Miliga-biga beach in Bulusan, Sorsogon, offer great potential for wave energy generation due to perceived high waves at the site. This study aims to assess the wave energy resource potential in the study area considering three different oscillating body wave energy converters (WEC). A Delft3D-WAVE model was setup off the coast of Sorsogon and ran under prevailing wind and wave conditions from January 1, 2018 to December 31, 2018. Validation with WaveWatch III model wave heights and periods at an offshore point within the numerical grid resulted to a root-mean-square-error of 0.205 m and 2.117 s, respectively, suggesting acceptable model accuracy. The prevailing wave direction in the study area is north-north-east with wave heights between 1 to 2 m and corresponding period between 5 to 7 s. This can reach up to 4 m and period of 10 s during peak northeast monsoon season. The annual average wave power density at the observation point, approximately 1 km off the study coast and around 80 m deep, was found to be 11.15 kW/m, which is sufficient for wave energy generation based on minimum threshold value from literature. The total annual harvestable energy was computed based on the wave resource matrix of the site and the specific power matrix of each WEC. It was found that one unit of a Floating 2-Body Heaving Buoy (F2-HB) can supply 960.706 MWh per year. The methodology conducted in this research can be applied for preliminary wave energy resource assessment at any potential site in the country.*

Keywords*: wave power, wave energy converter, wave modelling, renewable energy, Delft3D-WAVE*

I. INTRODUCTION

The Philippines' geographic location grants it a diverse and exceptional potential for renewable energy, including geothermal, hydro, solar, wind, and ocean resources, contributing approximately 22% to the country's total power generation mix as of 2022 [1]. This is composed of geothermal (10%), hydropower (9%), solar (2%), wind (1%) and biomass (1%). Ambitious government targets, notably from the National Renewable Energy Program (NREP), updated the goal to increase the installed renewable capacity to 35% of the power mix by 2030 and to 50% by 2040 [2]. Among the sources of renewable energy in the mix, the country's ocean energy resource has not been fully utilized. Energy from the ocean can be harnessed either from tide elevation difference, tidal currents, thermal gradient, and waves [3]. Local studies on ocean energy are mostly exploratory and scattered on various potential sites around the country. Palconit et al. (2021) assessed the potential tidal stream power in Pakiputan

Strait, Davao Gulf and estimated an annual energy production of 1350 kWh/year [4]. In Dinagat Islands, Caquilala et al. (2023) conducted a techno-economic assessment of various tidal current devices and found Evopod E1000 as the best device with indicative potential capacity of 140,000 kW with 0.16$/kWh cost of energy [5]. Villalba et al. (2021) simulated the tidal currents between various islands in the Visayas and Mindanao region and identified Banug strait as the area with the most energy density of 253.2 kWh/m^2 [6]. On the other hand, 15 sites all over the country were identified as potential for ocean thermal energy resource based on extensive temperature measurements [7]. The country is also not lacking in terms of wave energy resource. The eastern coast, facing the Pacific Ocean, is exposed to prevailing waves that are high and long enough for energy harnessing as detailed from the studies of Galano and De Leon (2024) [8], Wang et al. (2023) [9], and Decapia et al (2025) [10] who did a preliminary wave energy resource assessment of the entire Philippines using various methods.

Wave energy resource assessment is usually done in two stages: wave climate characterization and wave power calculation. The wave climate in a particular area can be characterized though global hindcast models such as WaveWatch III or satellite altimetry data [3, 8, 9, 10]. However, these datasets are often coarse in terms of spatial and temporal resolution limiting their applicability to regional analysis only. An alternative is to perform numerical simulation using a wave model such as Simulating Waves Nearshore (SWAN) or MIKE 21 Spectral Wave (SW). These models account for various nearshore wave processes and ideal to use in describing the wave conditions of a particular area [11]. Once the wave climate is characterized, the wave height and period are then processed to estimate the wave energy density and/or wave power density using an established formula from literature. If a specific wave energy converter (WEC) is considered, the wave resource matrix is multiplied to the power matrix of the WEC to obtain the wave energy matrix, which when summed, will yield the total harvestable wave energy [3, 8]. As most local studies are still in the exploratory stage of wave energy resource assessment, the use of numerical modelling is not yet fully utilized for a particular site. The study of Decapia et al. (2025), used SWAN and satellite altimetry for validation to characterize the wave climate at Baler, Aurora and estimate its wave energy resource potential but a specific WEC was not investigated in the study [10]. On the other hand, Paculdo et al. (2022), used SWAN to assess the wave energy resource on Cuyo Island, Palawan as an alternative source of electricity at the off-grid island. Three WECs, namely Wave Dragon, Archimedes WaveSwing (AWS), and Sea Slot-cone Generator (SSG), were considered in the assessment and resulted to a low-capacity factor of 3.4% due to relatively calm wave climate surrounding the island [12]. This is also the case in the study of Aminudin et al. (2021) where they used Mike 21 SW to simulate nearshore wave conditions at the coast of Dumaran, Palawan [13]. Despite the use of numerical modelling in these studies, the potential wave energy resource that is applicable for industry-scale implementation did not manifest because of unfavorable wave conditions.

Despite the country's recognized ocean energy potential, wave energy development in the country remains constrained by the limited number of site-specific studies and the largely exploratory nature of existing assessments. The research gap lies in the limited application of validated numerical wave models for preliminary wave energy resource assessment in the Philippines, particularly for linking site-specific wave conditions with the performance of

specific WECs. This study addresses that gap by applying a validated Delft3D-WAVE model to a Pacific-facing site in Bulusan, Sorsogon. This would link the resulting wave resource characterization at the study site with the performance matrices of selected point absorber WECs to evaluate their respective energy harvesting potential. This study is significant as the methodology conducted in this research can be adopted for preliminary assessment of wave energy resource at any location in the Philippines.

II. METHODOLOGY

2.1 Study Site

The study site for this research is the area off the coast of Miliga-biga beach, Bulusan, Sorsogon shown in Figure 1. It is located at Barangay Mabuhay, Bulusan, Sorsogon, a coastal barangay southeast of Bulusan facing the Pacific Ocean. The 500-meter beach is located at 12º43'56" N latitude and 124 º 07'55" E longitude. This site was selected because it is widely recognized within the municipality of Bulusan as one of the most energetic wave environments along the local coastline due to its direct exposure to the Pacific Ocean [3]. The site was previously used for surfing, indicating the presence of consistently strong waves, but it has also been regarded by local residents as hazardous for swimming and recreation due to incidents of drowning associated with its rough sea conditions. In addition, local fishers generally avoid operating in the area because of the turbulent wave climate, further suggesting that the site experiences persistently energetic nearshore conditions. Its orientation toward the open Pacific, combined with the influence of seasonal monsoons, makes the beach highly exposed to both locally generated wind waves and incoming ocean swell, making it a strong candidate for wave energy resource assessment. During the northeast monsoon (Amihan) from November to March, prevailing winds generate tall, steady waves from the northeast direction. In contrast, the southwest monsoon (Habagat) from June to October brings relatively calmer waves but still creates a dynamic sea state. The coastline is also exposed to long-period swells generated by distant weather systems in the Pacific Ocean, which can arrive regardless of the local monsoon season.

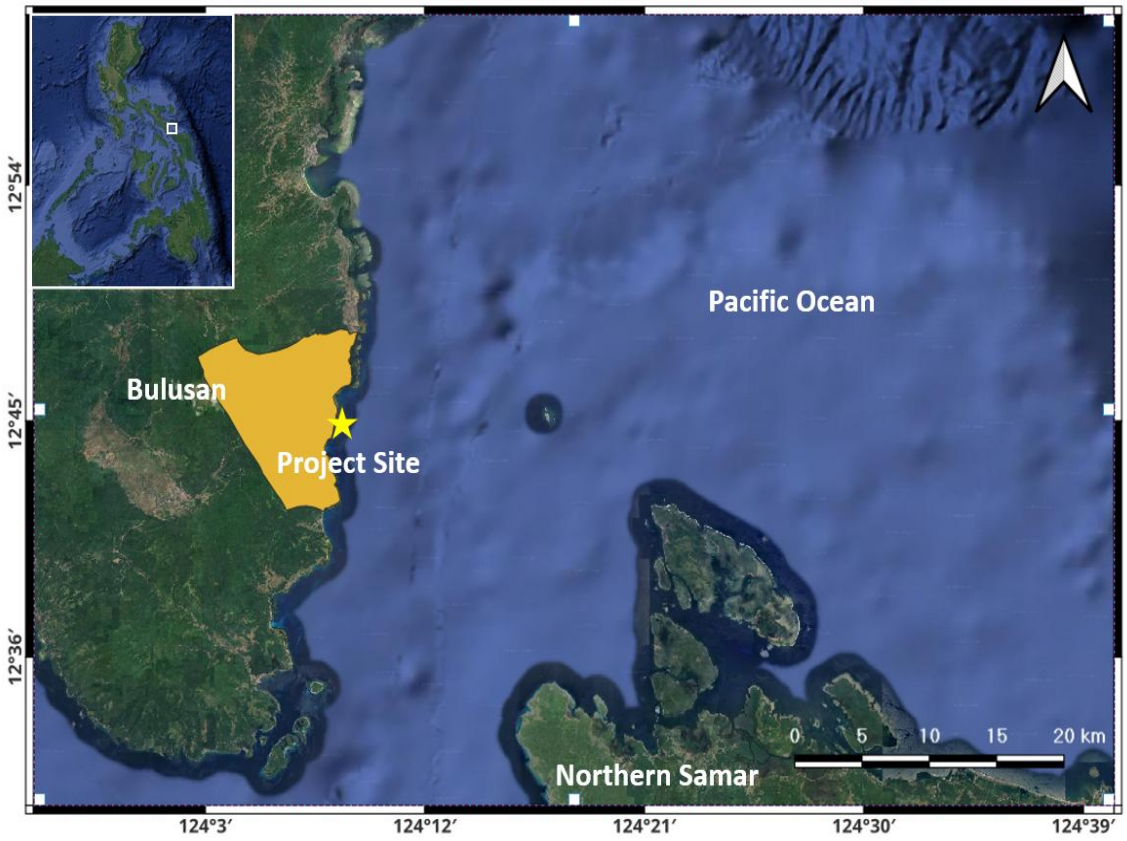

Figure 1. Study site location (*Source: Google Earth*)

2.2 Data Collection

This research only utilized secondary data from various global datasets. Details of each data collected are discussed in the succeeding subsections and are summarized in Table 1.

2.2.1 Bathymetry

The bathymetry of the study area was downloaded from the General Bathymetric Chart of the Oceans (GEBCO) global dataset. GEBCO is a foundational international program dedicated to mapping the entire ocean floor operated under the joint efforts of the International Hydrographic Organization (IHO) and the Intergovernmental Oceanographic Commission (IOC) of UNESCO, guiding its global mission. It provides a continuous, global digital bathymetric model at a 15-arc second resolution, or roughly translates to 450 meters, depicting the shape and depth of the seabed worldwide [14]. This data was used as model input to the numerical model.

2.2.2 Wind

Wind data was downloaded from the European Centre for Medium-Range Weather Forecasts Earth Reanalysis 5th generation (ECMWF ERA5) global data set. ERA5 is the fifth generation of atmospheric reanalysis data from the ECMWF, providing a comprehensive, global record of the climate from 1940 to the present. It combines vast amounts of historical observations with advanced modeling to produce highly detailed estimates of atmospheric,

land, and oceanic climate variables [15]. ERA5 provides hourly values of wind data on a global grid with a spatial resolution of 0.25° x 0.25°. As the wave processes simulated are offshore, local wind data from PAGASA, which comes from an inland weather station, was not utilized in this study.

2.2.3 Wave

Two wave datasets were downloaded for this study. The first one, from ERA5 dataset, was downloaded at the point 13.5º N latitude and 125.5º E longitude and was used as the time-varying boundary conditions for the computational domain. The second data set was from WaveWatch III developed by National Oceanic and Atmospheric Administration (NOAA). It is a third-generation spectral wave model that simulates the generation, propagation, and interaction of wind-generated ocean waves on a global or regional scale [16]. The spatial resolution of WaveWatch III data is 0.5º x 0.5º so the closest point to the study area is located at 13º N latitude and 125º E longitude. Unlike ERA5 wave data that has an hourly temporal resolution, WaveWatch III data are published every 3 hours. These data were used to validate the results of the numerical model simulation. Although using wave data from an offshore buoy is ideal for validation, there is no available data near the study site from any local institution, including NAMRIA and PAGASA.

Table 1. Summary of data collected

Data	Source	Spatial Resolution	Temporal Resolution
Bathymetry	GEBCO (2019)	15-arc second	None
Wind	ECMWF ERA5	0.25º by 0.25º	Hourly
Wave (Boundary)	ECMWF ERA5	0.5º by 0.5º	Hourly
Wave (Validation)	NOAA WaveWatch III	0.5º by 0.5º	3-hourly

2.3 Numerical Model

This study used the Delft3D modelling suite, an integrated system consists of a number of modules, developed by Deltares in close cooperation with Delft University of Technology. In this study, only the wave model, Delft3D-WAVE was utilized. The module is based on the program, Simulating Waves Nearshore (SWAN), and is a third-generation spectral wave model used in simulating random, short-crested wind-generated waves in estuaries, tidal inlets, lakes, among others. SWAN is based on the discrete spectral action balance equation action balance equation that describes the rate of change of the wave action density at a single point in space and relating it to the physical processes which generate, dissipate, or redistribute wave energy, given by sources and sinks. SWAN solves the discrete spectral action balance equation using an implicit upwind finite difference scheme in five dimensions (time, physical space, and spectral space) on a structured grid [11].

2.4 Model Set-up

2.4.1 Computational Domain

The computational domain used in this study is a tilted rectangular grid that extends up to the deeper portions of the Pacific Ocean. It is composed of 91 by 109 nodes and has a resolution of 1 km by 1 km. The bathymetry from GEBCO was incorporated into the numerical grid but

elements that have a negative depth were removed as they represent land. Two observation points were defined at the study area. The first one is located 1 km offshore from the beach at 80 m depth and the other at 13° N latitude and 125° E longitude which serves as validation point for the model. Time-series wave data from the numerical simulation were stored at these observation points and shall be used for analysis and validation. Figure 2 shows the computational domain used in this study.

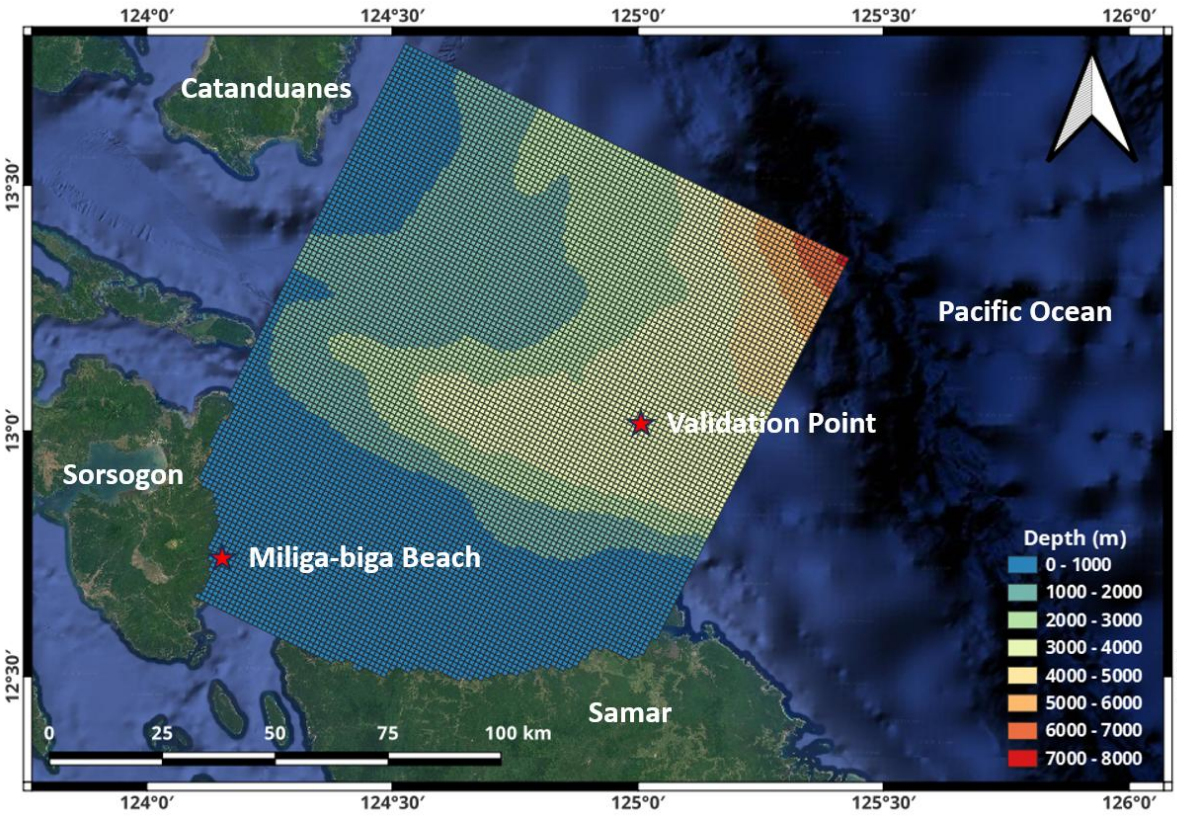

Figure 2. Model computational domain

The spectral resolution of the numerical grid was set to all spectral directions covering a full circle while the range of frequencies to be included in the model simulation is from 0.05 to 1 Hz. Both settings were the default options in Delft3D-WAVE.

2.4.2 Time Frame and Boundary Conditions

The time frame used in the simulation lasted for a full year from January 1, 2018 00:00:00 UTC to December 31, 2018 23:00:00 UTC to account for seasonal variations within a year, i.e. northeast and southwest monsoons. Longer simulation period that can account for interannual variability was not performed in the study due to limitation in computational capacity. The simulation time step is hourly, following the temporal resolution of the wave data at the model boundaries. The model was run in non-stationary mode as the time for the waves to propagate from the boundaries to the study site is significantly larger than the set time step of 60 minutes [17].

The incident wave conditions along the open boundaries of the computational grid were defined at the north and east orientation of the model domain. Values for wave parameters along the boundary conditions were specified from the downloaded ERA5 data. In the absence of higher resolution wave data, the time-varying significant wave height, peak period, and mean direction were applied uniformly across the boundaries where the depth is at least 5 m. These parameters, along with a constant directional spreading of 5 (power of cosine), indicating broad spread of wind waves, were used to generate a theoretical JONSWAP spectrum, with a default peak enhancement factor of 3.3, that will propagate into the model domain.

Hydrodynamic conditions such as water level and current velocity directly influence wave height, direction, and energy through processes like wave–current interaction and tidal modulation [18]. However, due to absence of available water level and velocity data, hydrodynamic conditions were set to zero throughout the entire simulation. While not ideal, this simplification is generally accepted for preliminary wave resource assessments to reduce the computational demand of the long-term simulation [19].

2.4.3 Physical Parameters and Processes

The default values for the hydrodynamic constants were applied in this research: 9.81 m/s^2 for gravitational acceleration and 1025 kg/m^3 for water density. Wind was applied into the model as a spatially-constant, time-varying parameter. Wind data from ERA5 at the point, 13ºN latitude and 125º E longitude were processed and the wind rose diagram is shown in Figure 3. In addition, the monthly time-series fluctuation of wind speed is shown in Figure 4. To account for wind growth, the wind drag parametrization of Wu (1982) was utilized since its linear formulation is highly accurate for moderate wind speeds which constitutes the prevailing wind conditions in the study site [20]. It is important to note that the study does not take into account specific extreme weather conditions since the objective of the study is to assess the wave energy resource. For such a study, prevailing wind conditions are more appropriate to check its reliability as it happens around 95% of the time [19]. The extreme weather condition scenario can be applied at the more detailed assessment when the structural stability of the WECs is the main concern.

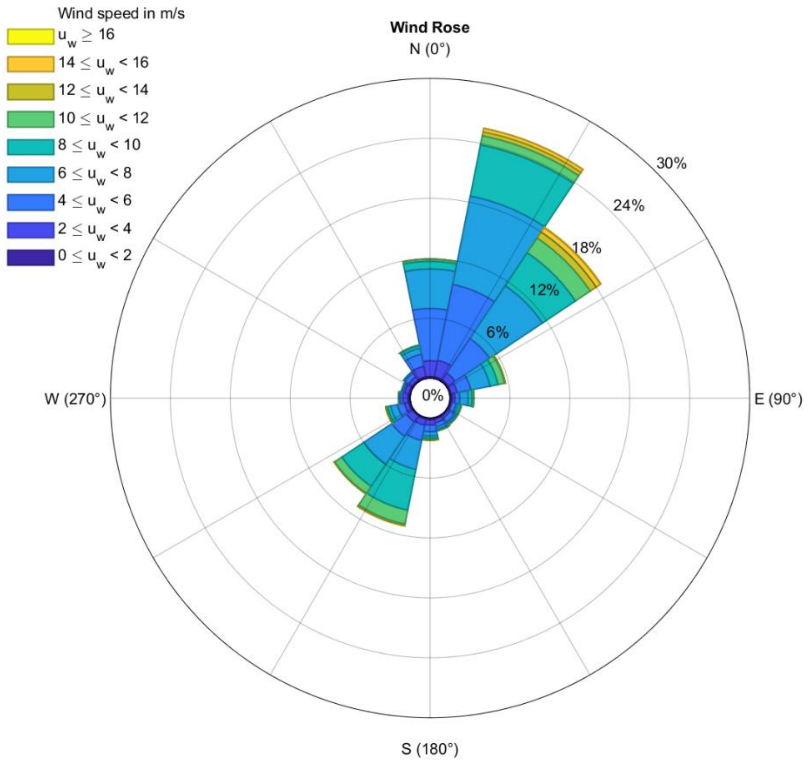

Figure 3. Wind rose diagram applied to model simulation

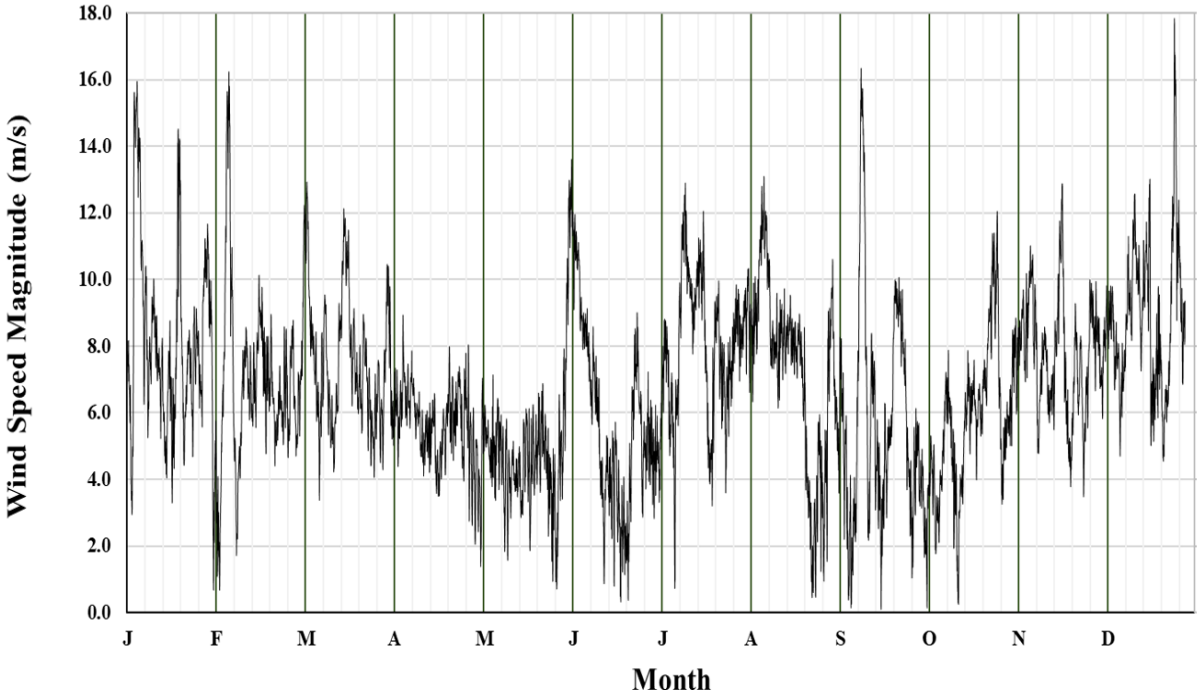

Figure 4. Time-series wind speed applied to model simulation

Besides wind growth, other processes activated in the model simulation are whitecapping, depth-induced breaking, non-linear triad interaction, bottom friction, and diffraction. Whitecapping controls deep-water energy dissipation, where a reduction in this value prevents the premature dampening of long-period swells essential for accurate resource mapping. In contrast, bottom friction and depth-induced breaking parameters primarily alters the nearshore significant wave height, as these settings determine how much energy is lost to the seabed or through surf-zone turbulence. Non-linear triad interactions and diffraction shift the spectral peak and redistribute energy around complex coastal features like headlands. For deep water, open sea Delft3D-WAVE applications like this study, whitecapping is the process that has the most effect on the simulated wave properties [21]. For this study, the formulation of Komen et al. (1994) was selected due to its proven stability in modeling fully developed wind-seas and its conservative dissipation of long-period Pacific swells, making it ideal for characterizing the prevailing monsoon-driven wave climate of the Philippine eastern seaboard [22].

2.5 Validation

The level of agreement between observed and modelled time-series data were assessed by calculating the root-mean-square error (RMSE), bias, and scatter index (SI). The period considered for validation is from January 1, 2018 to May 1, 2018 when the waves are more active because of the northeast monsoon. The formulas for RMSE, bias, and SI are shown in Equations 1, 2, and 3, respectively.

$$RMSE = \sqrt{\frac{1}{N}\sum_{i=1}^{N} (S_i - O_i)^2} \tag{1}$$

$$bias = \sum_{i=1}^{N} \frac{1}{N}(S_i - O_i)^2 \tag{2}$$

$$SI = \frac{\sqrt{\frac{1}{N}\sum_{i=1}^{N} (S_i - O_i)^2}}{\frac{1}{N}\sum_{i=1}^{N} O_i} \times 100 \tag{3}$$

where N is the total number of data points, S_i is the simulated data, and O_i is the observed data which corresponds to the WaveWatch III data.

Williams and Estevez (2017) recommended statistical guidelines to establish calibration standards for a minimum level of performance for coastal and estuarine models [23]. Results of the model validation are summarized in Table 2 and visualized in Figures 5 to 7. Based on

the statistical parameters calculated, the wave model can be considered to simulate the wave processes in the domain excellently.

Table 2. Results of model validation

Statistical Parameter	Quality Index	Hs (m)		Tp (s)	
		Threshold [19]	Modelled	Threshold [19]	Modelled
RMSE	Accuracy	0.215	0.171	1.931	0.449
Bias	Bias	0.15	0.03	0.20	0.20
SI	Agreement	10	8.0	20	4.7

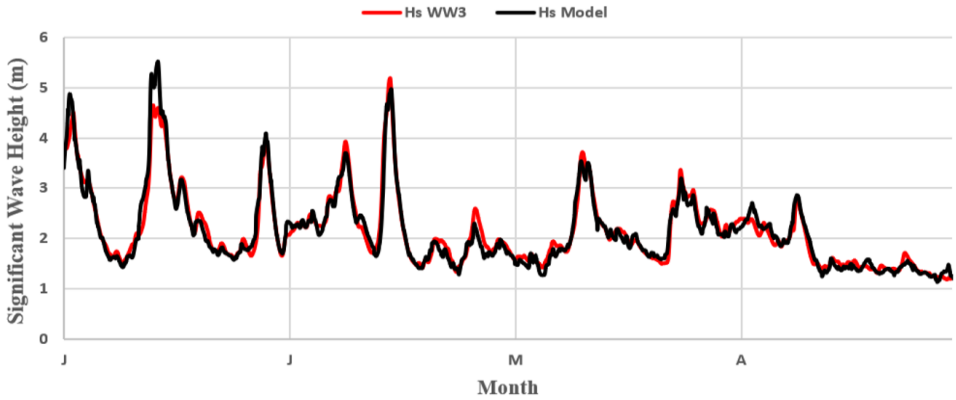

Figure 5. Comparison of simulated (black) and downloaded (red) significant wave height at validation point

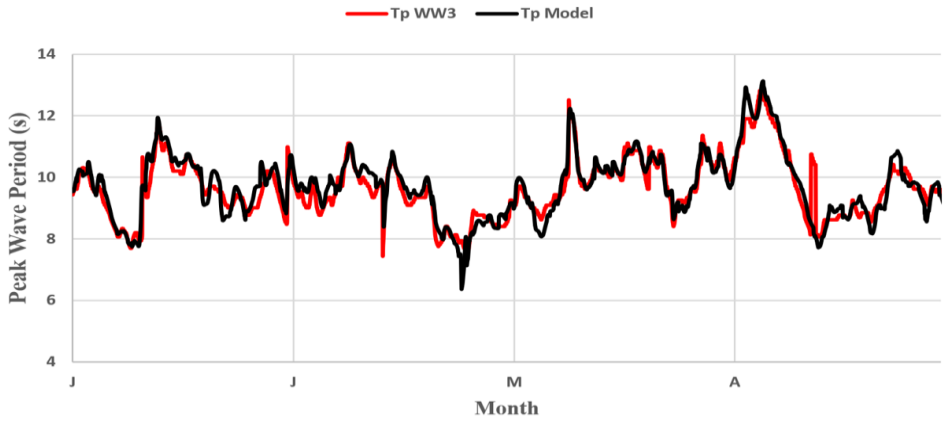

Figure 6. Comparison of simulated (black) and downloaded (red) peak wave period at validation point

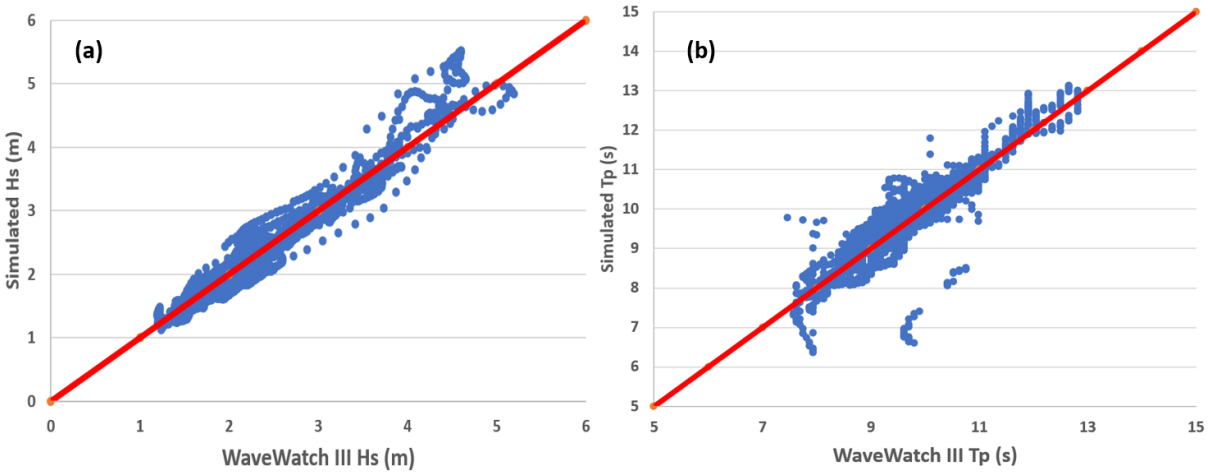

Figure 7. Scatter diagram showing the relationship between modelled and WW3 (a) significant wave height and (b) peak period at validation point

2.6 Wave Energy Resource Assessment

An initial assessment of the feasibility of WEC installation in a particular area can be based on the wave power density given by Equation 4. If the mean annual wave power density at a particular site is more than the standard benchmark of 5 kW/m, it can be considered as wave energy resource [24].

$$P_w = \frac{\rho g^2 H_s^2 T_p}{64\pi} \tag{4}$$

where P_w is the wave power density in W/m, ρ is the density of seawater in kg/m^3, g is the acceleration due to gravity in m/s^2, H_s is the significant wave height in m, and T_p is the peak wave period in s.

In addition, the seasonal variability (SV) index, given by Equation 5, is a parameter used to assess the temporal reliability of waves on a proposed wave energy resource site. In general, a site with a moderate but steady resource can be more attractive than a site with a high average power that is or only available during certain seasons. Ideally, a viable site has an SV value of less than 1.0 [25].

$$SV = \frac{P_{S1} - P_{S4}}{P_{year}} \tag{5}$$

where SV is the seasonal variability index, P_{S1} is the mean wave power during the most energetic season in kW, P_{S4} is the mean wave power during the least energetic season in kW, and P_{year} is the mean wave power during the entire year in kW.

2.7 Wave Energy Converters

Wave energy converters (WEC) are devices that convert the kinetic energy from waves into electrical energy. There are different types of WEC based on its principle of conversion including oscillating water column, oscillating body devices, overtopping, and attenuators, among others. This study will focus on oscillating body devices particularly the following buoy-type WEC discussed in Carballo et al. (2019): AquaBuoy, Bottom-Referenced Heaving Buoy (BREF-HB), and Floating Two-body Heaving Buoy (F2-HB). These were selected because they are point absorber WECs, a class of devices recognized for their compact size, relatively simple design, and ability to absorb energy from waves approaching from different directions. These characteristics make point absorbers suitable for preliminary site-level assessment. In addition, the power matrices of these devices are available in the literature [26], enabling direct estimation of harvestable energy from the simulated wave resource matrix at the study site. AquaBuoy works through vertical mechanical movement due to waves. This vertical movement consequently drives movement of a buoyant disk contained within a vertical tube or cylinder which in turn creates piston motion. The created water piston then pressurizes the water contained within a hose due to repeated elongation and relaxation, thus acting as a generator [26]. BREF-HB also works through the vertical motion of waves but also generates energy through horizontal translation due to wave propagation. It consists of a floating axisymmetric buoy with ellipsoidal cross section which is connected by a wire to a machinery unit situated at the bottom of the sea. The machinery unit is composed of a linear generator placed inside a steel hull mounted on a concrete ballast. The wave action generates a pull to the wire then drives the linear generator [27]. F2-HB works through vertical motion of waves as well as through horizontal translation due to wave propagation. The device consists of two main components, a floating buoy, and a sliding torus. Wave energy is generated by relative motion of these two components through hydraulic power take-off system [27]. Figure 8 shows the schematic diagram of the three wave energy converters considered in this study.

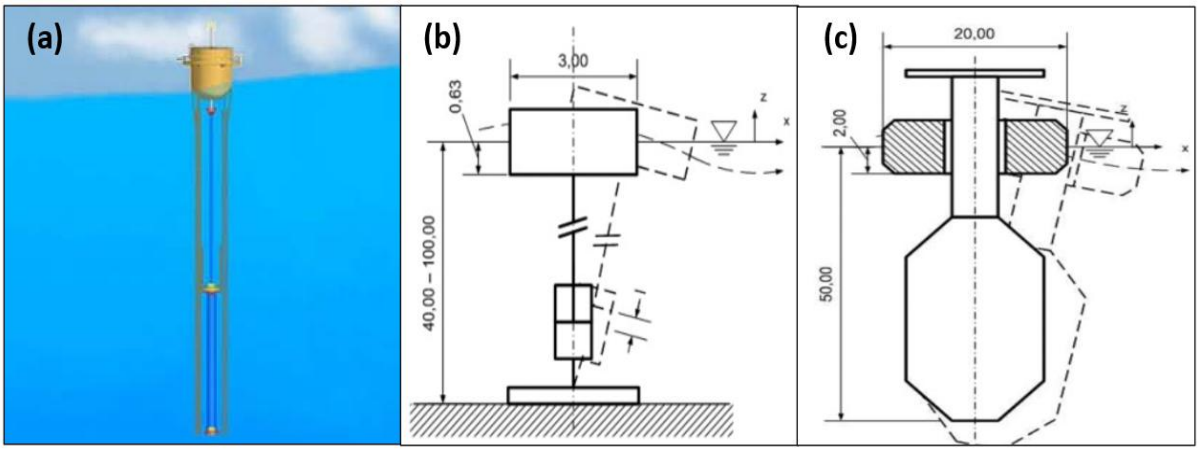

Figure 8. Schematic diagram of (a) AquaBuoy, (b) BREF-HB, and (c) F2-HB WEC

In estimating the wave energy that can be harvested by a specific WEC, the main reference considered is its power matrix. A power matrix is a standardized table used to characterize the performance of a WEC by mapping the expected electrical power output of a specific device

across a range of different ocean conditions. Figures 9, 10, and 11 show the power matrices of AquaBuoy, BREF-HB, and F2-HB, respectively [26]. A wave resource matrix, on the other hand, shows the number of times a particular wave of height, H_s, with corresponding period, T_p, propagate at a certain point. By combining a WEC's power matrix with the wave resource matrix, the total annual harvestable energy can be estimated using Equation 6.

$$Total\ annual\ harvestable\ energy\ in\ kWh = \sum_{i=1}^{n} P_i F_i \Delta t \tag{6}$$

where P_i is the power output of the WEC from its power matrix in kW, F_i is the frequency of occurrence of a particular wave property from the wave resource matrix, Δt is the time interval between wave data in hrs, and n is the number of data points analyzed.

		Tp (s)												
		0-1.0	1.0-2.0	2.0-3.0	3.0-4.0	4.0-5.0	5.0-6.0	6.0-7.0	7.0-8.0	8.0-9.0	9.0-10.0	10.0-11.0	11.0-12.0	12.0-13.0
Hs (m)	0-0.5	0	0	0	0	0	0	0	0	0	0	0	0	0
	0.5-1.0	0	0	0	0	0	0	8	11	12	11	10	8	7
	1.0-1.5	0	0	0	0	0	13	17	25	27	26	23	19	15
	1.5-2.0	0	0	0	0	0	24	30	44	49	41	41	34	28
	2.0-2.5	0	0	0	0	0	37	47	69	77	73	64	54	43
	2.5-3.0	0	0	0	0	0	54	68	99	111	106	92	77	63
	3.0-3.5	0	0	0	0	0	0	93	135	152	144	126	105	86
	3.5-4.0	0	0	0	0	0	0	0	122	176	198	188	164	137
	4.0-4.5	0	0	0	0	0	0	0	223	250	239	208	173	142
	4.5-5.0	0	0	0	0	0	0	0	250	250	250	250	214	175
	5.0-5.5	0	0	0	0	0	0	0	250	250	250	250	250	211

Figure 9. AquaBuoy Power Matrix [26]

		Tp (s)												
		0-1.0	1.0-2.0	2.0-3.0	3.0-4.0	4.0-5.0	5.0-6.0	6.0-7.0	7.0-8.0	8.0-9.0	9.0-10.0	10.0-11.0	11.0-12.0	12.0-13.0
Hs (m)	0-0.5	0	0	0	0	0	0	0	0	0	0	0	0	0
	0.5-1.0	0	0	0	1.2	1.3	1.2	1.2	1.1	1	0.9	0.8	0.7	0.7
	1.0-1.5	0	0	0	2.6	2.5	2.3	2.2	2.3	2	1.9	1.7	1.4	1.5
	1.5-2.0	0	0	0	4.4	4	3.7	3.6	3.5	3.1	2.8	2.5	2.3	2.2
	2.0-2.5	0	0	0	0	6	5.2	4.5	4.6	4.3	3.9	3.6	3	2.8
	2.5-3.0	0	0	0	0	7.4	6.7	6.2	5.7	5.4	4.7	4.1	4.1	3.7
	3.0-3.5	0	0	0	0	0	8.4	7.3	6.9	5.8	5.4	4.9	4.4	4.2
	3.5-4.0	0	0	0	0	0	8.9	8.6	7.6	6.8	6.2	5.6	5	4.6
	4.0-4.5	0	0	0	0	0	10.6	9.5	8.7	7.6	7	6.1	5.9	5.4
	4.5-5.0	0	0	0	0	0	12.2	11.1	9.2	8.6	7.3	7.2	6.3	5.9
	5.0-5.5	0	0	0	0	0	0	13.1	10.1	8.9	8.1	7.5	6.8	6.4

Figure 10. BREF-HB Power Matrix [26]

		Tp (s)												
		0-1.0	1.0-2.0	2.0-3.0	3.0-4.0	4.0-5.0	5.0-6.0	6.0-7.0	7.0-8.0	8.0-9.0	9.0-10.0	10.0-11.0	11.0-12.0	12.0-13.0
Hs (m)	0-0.5	0	0	0	0	0	0	0	0	0	0	0	0	0
	0.5-1.0	0	0	0	6	11	19	25	30	44	50	53	44	34
	1.0-1.5	0	0	0	13	25	43	55	68	90	102	92	91	66
	1.5-2.0	0	0	0	24	45	65	100	121	153	175	151	122	126
	2.0-2.5	0	0	0	0	65	137	205	244	357	293	353	260	248
	2.5-3.0	0	0	0	0	96	137	205	244	357	293	353	260	248
	3.0-3.5	0	0	0	0	0	192	254	291	431	385	424	314	285
	3.5-4.0	0	0	0	0	0	256	366	403	551	536	531	473	420
	4.0-4.5	0	0	0	0	0	327	418	574	678	708	665	509	415
	4.5-5.0	0	0	0	0	0	358	514	658	824	828	618	638	512
	5.0-5.5	0	0	0	0	0	0	610	774	880	936	905	805	603

Figure 11. F2-HB Power Matrix [26]

III. RESULTS AND DISCUSSION

3.1 Wave Climate

The wave climate in the study area is governed primarily by wind with heights varying between 1 m to 3 m and periods of 4 s to 8 s, as shown in Figures 12 and 13. This reaches up to 4 m and 10 s during peak northeast monsoon or Amihan season. As seen in the wave rose diagrams of Figures 14 and 15, the prevailing wave direction all throughout the year is from north-north-east. Waves during southwest monsoon or Habagat season are generally calmer as the open sea is to the east of the study area. Land masses block the path of the wind and its opposite direction with respect to the wave propagation causes decay in the properties of the waves. During northeast monsoon season and easterlies, the prevailing wind promotes wave growth as it blows along the direction of the wave propagation. Figures 16 and 17 show the monthly average significant wave height and peak wave period at the study site, exhibiting further the effect of the monsoon season to the wave climate.

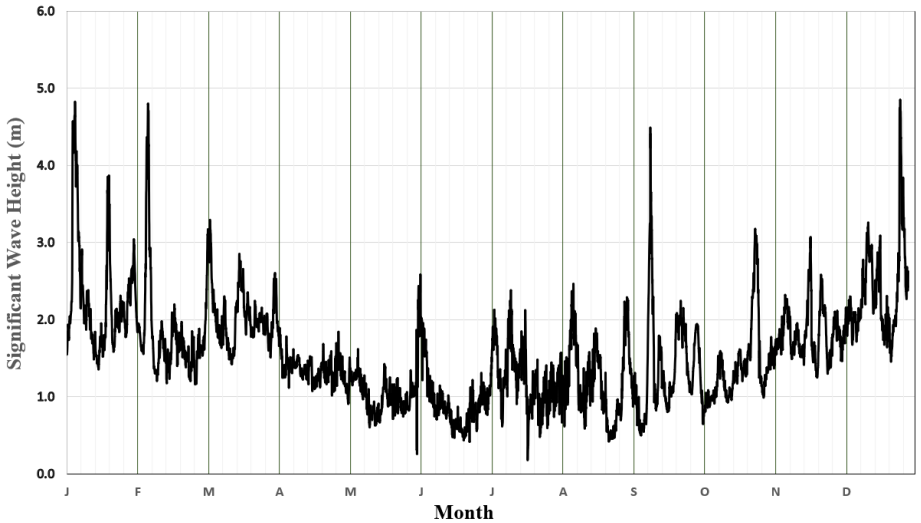

Figure 12. Simulated hourly significant wave height at the study area

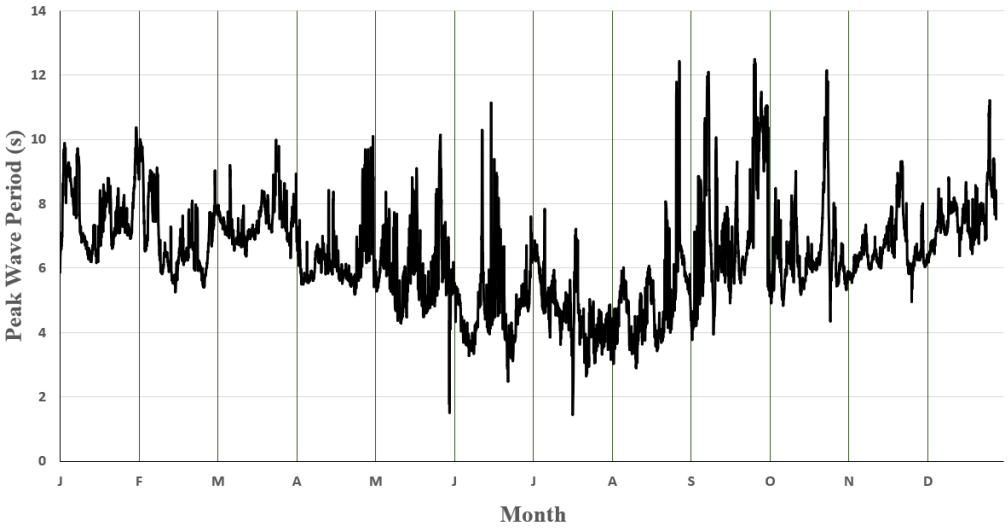

Figure 13. Simulated hourly peak wave period at the study area

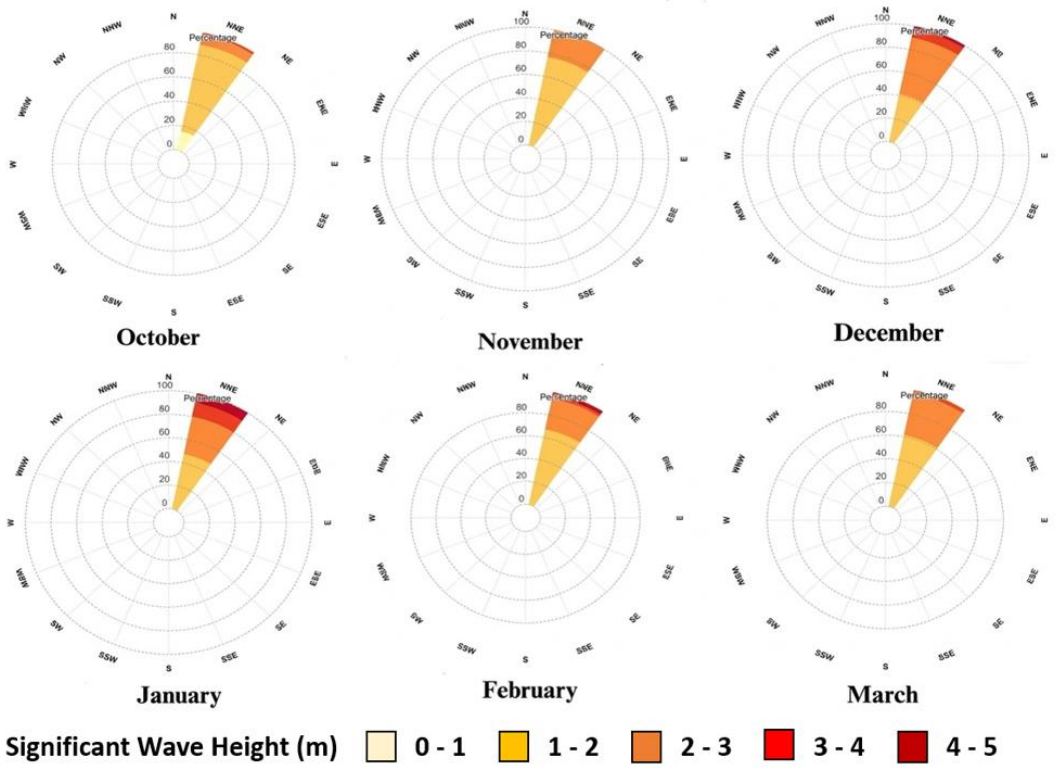

Figure 14. Wave rose diagrams at study area from during Amihan months

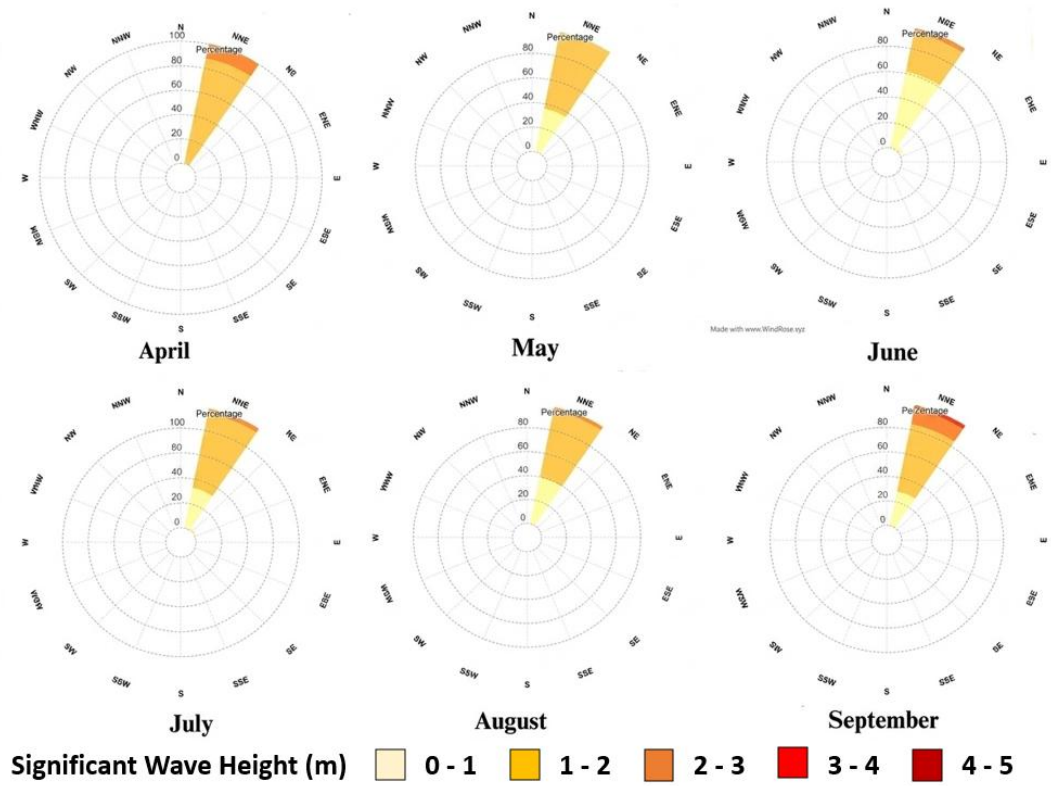

Figure 15. Wave rose diagrams at study area from during Habagat months

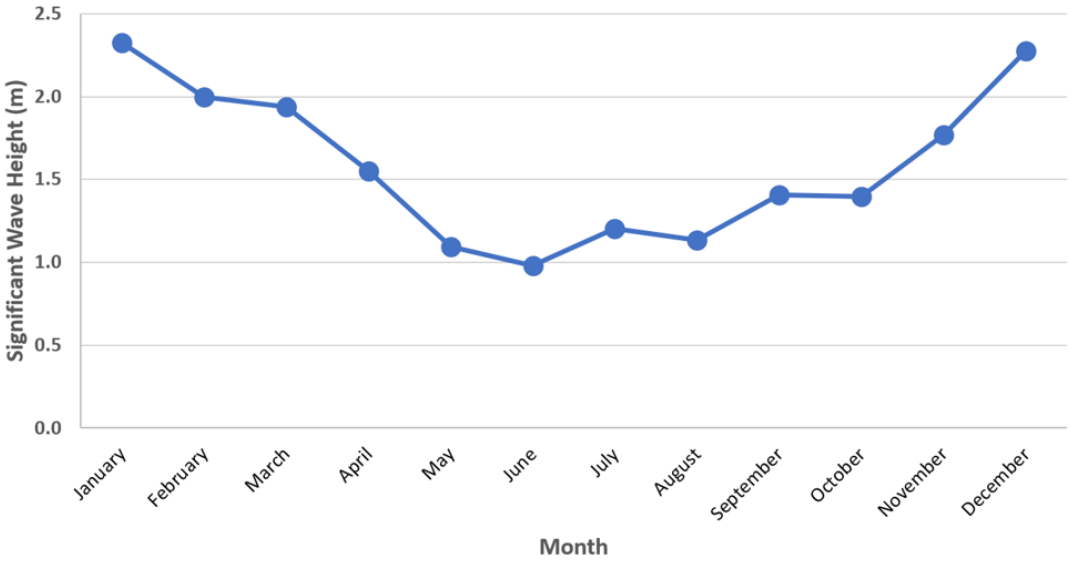

Figure 16. Simulated monthly average significant wave height at study area

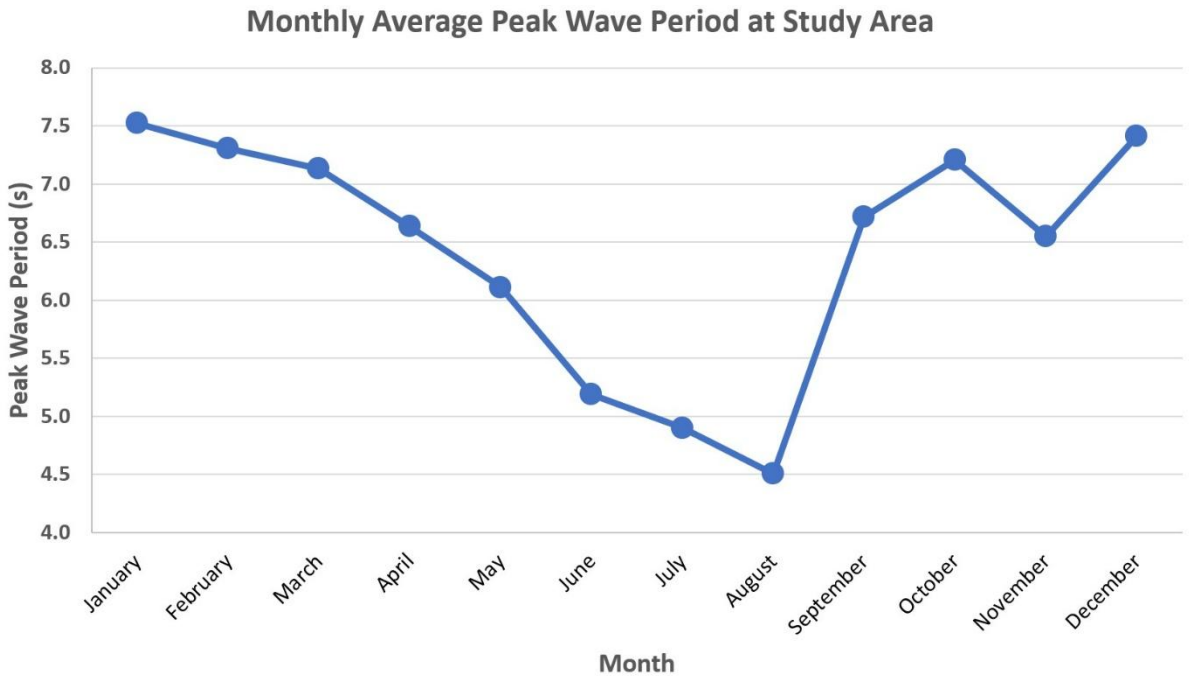

Figure 17. Simulated monthly average peak wave period at study area

The simulated hourly significant wave height and peak wave period were processed to derive the wave resource matrix at the study site. For each time step, the wave height and period were categorized and tallied to its corresponding cell in the matrix shown in Figure 17. Most of the waves that propagate at the study area have a significant wave height of 1 to 2 m with corresponding period of 5 to 7 s. This signifies that the waves are mostly wind-generated having a frequency between 0.1 to 0.5 Hz.

		Wave Resource Matrix at Study Area												
		Tp (s)												
		0-1.0	1.0-2.0	2.0-3.0	3.0-4.0	4.0-5.0	5.0-6.0	6.0-7.0	7.0-8.0	8.0-9.0	9.0-10.0	10.0-11.0	11.0-12.0	12.0-13.0
Hs (m)	0-0.5	0	6	7	1	8	10	19	16	5	0	0	2	0
	0.5-1.0	0	0	14	389	387	333	179	117	78	31	22	10	0
	1.0-1.5	0	0	0	77	627	875	668	248	95	58	19	6	11
	1.5-2.0	0	0	0	0	96	490	1212	531	140	88	31	7	0
	2.0-2.5	0	0	0	0	0	85	328	458	130	105	13	6	0
	2.5-3.0	0	0	0	0	0	0	39	241	82	21	4	9	1
	3.0-3.5	0	0	0	0	0	0	7	74	37	0	17	12	4
	3.5-4.0	0	0	0	0	0	0	0	12	52	6	0	0	0
	4.0-4.5	0	0	0	0	0	0	0	1	56	15	0	0	0
	4.5-5.0	0	0	0	0	0	0	0	0	19	13	0	0	0

Figure 18. Wave resource matrix at the study area

3.2 Wave Energy Resource Viability

The hourly wave power density at the study area was calculated using Equation 4 and is shown in Figure 19. The red line indicates the 5 kW/m threshold by Mørk et al. (2020) where wave energy harvesting is deemed feasible. Based on simulation results, the annual mean power density was calculated at 11.15 kW/m, signifying the feasibility of installation of WEC at the study area.

The reliability of the available wave energy was assessed by calculating the SV index shown in Equation 5. According to Figure 19, the most energetic months are observed from December to February with a mean power density of 20.65 kW/m while the least energetic months are from June to August with a mean power density of 3.45 kW/m. This translates to an SV index value of 1.54, representing moderate viability of the wave energy resource [28]. The rate of exceedance for each month with respect to the minimum threshold value of 5 kW/m was also determined to further assess reliability. This parameter is expressed as a percentage of the time the minimum threshold value was equaled or exceeded. As shown in Figure 20, the period from November to April almost always exceeds the threshold of 5 kW/m. This is the ideal period suggested for an installed WEC to be fully operational. On the other hand, the months of May to August did not reach 50% reliability, meaning the wave power density at the study area during these months are less than 5 kW/m, less than 50% of the time.

Despite the unideal reliability of the wave energy resource, the study site can still be considered for wave energy harnessing due to the annual mean power density of 11.15 kW/m exceeding the 5 kW/m benchmark [24]. This value may still be high enough to justify the investment despite low production during the least energetic season. Other options can also be explored to address this issue. Seasonal deployment can be used as an alternative to target the high energy seasons [29]. Furthermore, hybridization, or making the study site to be a hybrid wind-wave energy farm, can be explored to maximize the deployment of such technology [30].

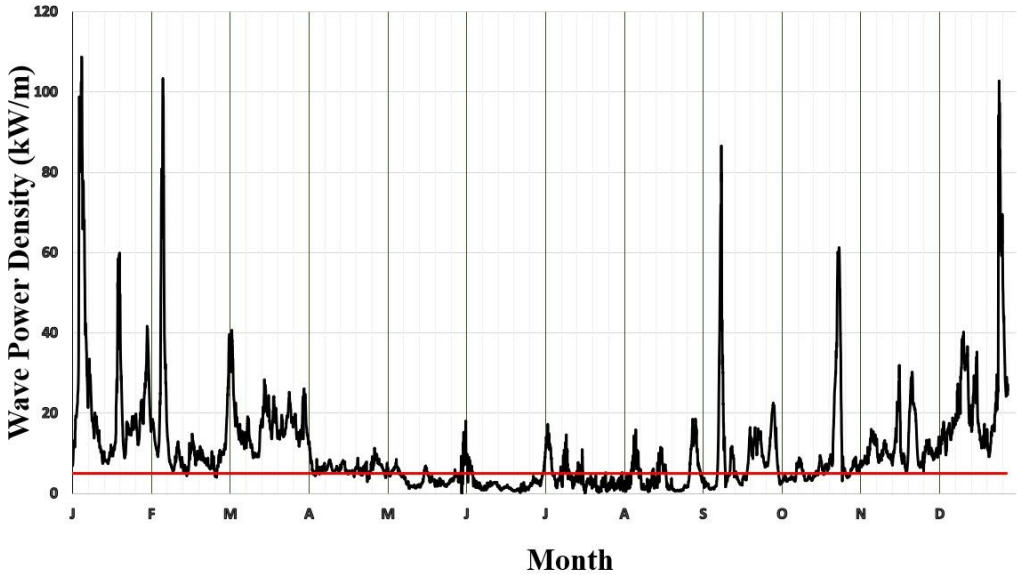

Figure 19. Simulated hourly wave power density at the study area
(red line shows the 5 kW/m threshold Mørk et al. (2020))

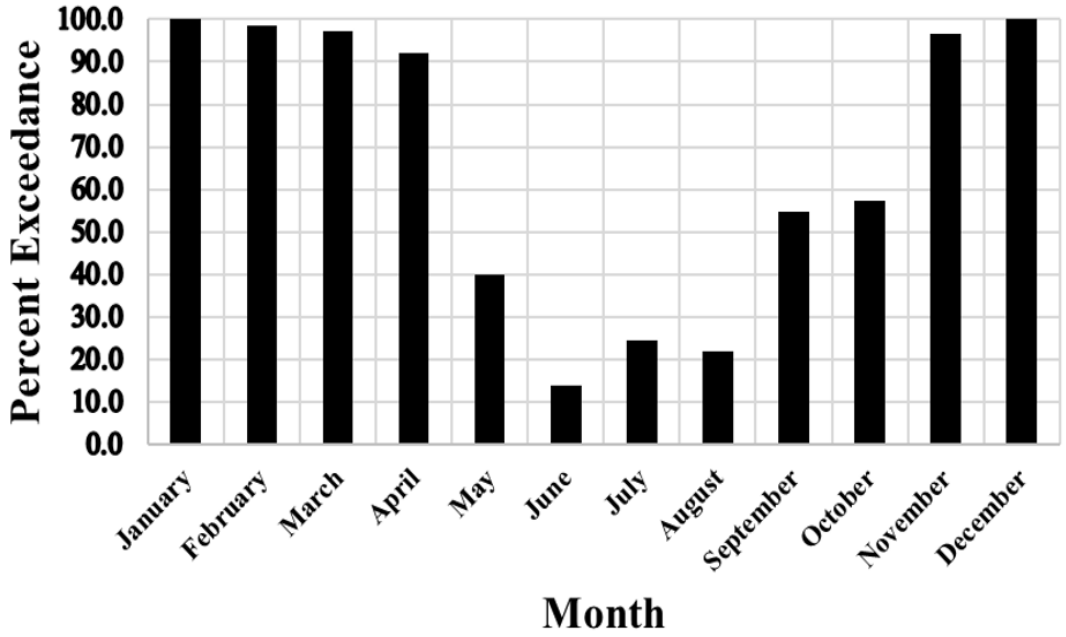

Figure 20. Monthly percent exceedance of the 5 kW/m threshold value of wave power density at the study area

3.3 Wave Energy Converter Assessment

The total annual harvestable wave energy for each WEC was computed by applying Equation 6. By multiplying the wave resource matrix in Figure 18 to each power matrix in Figures 9, 10, and 11, the matrix of harvestable wave energy for each WEC considered were obtained and are shown in Figures 21, 22, and 23. The total annual harvestable wave energy for each WEC, shown in Table 3, was obtained by summing all entries on each WEC's matrix. Based on obtained results, F2-HB yielded the most amount of harvestable wave energy among the 3 WECs considered due to the larger values in the power matrix of F2-HB that are within the most frequent wave conditions in the study area. This is sufficient to power around 1,500 households, or 24% of the municipal population, that are consuming 50 kW-hr monthly in the rural coastal areas where electricity is scarce [31].

		Tp (s)												
		0-1.0	1.0-2.0	2.0-3.0	3.0-4.0	4.0-5.0	5.0-6.0	6.0-7.0	7.0-8.0	8.0-9.0	9.0-10.0	10.0-11.0	11.0-12.0	12.0-13.0
Hs (m)	0-0.5	0	0	0	0	0	0	0	0	0	0	0	0	0
	0.5-1.0	0	0	0	0	0	0	1432	1287	936	341	220	80	0
	1.0-1.5	0	0	0	0	0	11375	11356	6200	2565	1508	437	114	165
	1.5-2.0	0	0	0	0	0	11760	36360	23364	6860	3608	1271	238	0
	2.0-2.5	0	0	0	0	0	3145	15416	31602	10010	7665	832	324	0
	2.5-3.0	0	0	0	0	0	0	2652	23859	9102	2226	368	693	63
	3.0-3.5	0	0	0	0	0	0	651	9990	5624	0	2142	1260	344
	3.5-4.0	0	0	0	0	0	0	0	1464	9152	1188	0	0	0
	4.0-4.5	0	0	0	0	0	0	0	223	14000	3585	0	0	0
	4.5-5.0	0	0	0	0	0	0	0	0	4750	3250	0	0	0
	5.0-5.5	0	0	0	0	0	0	0	0	0	0	0	0	0

Figure 21. AquaBuoy harvestable wave energy matrix

		Tp (s)												
		0-1.0	1.0-2.0	2.0-3.0	3.0-4.0	4.0-5.0	5.0-6.0	6.0-7.0	7.0-8.0	8.0-9.0	9.0-10.0	10.0-11.0	11.0-12.0	12.0-13.0
Hs (m)	0-0.5	0	0	0	0	0	0	0	0	0	0	0	0	0
	0.5-1.0	0	0	0	466.8	503.1	399.6	214.8	128.7	78	27.9	17.6	7	0
	1.0-1.5	0	0	0	200.2	1567.5	2012.5	1469.6	570.4	190	110.2	32.3	8.4	16.5
	1.5-2.0	0	0	0	0	384	1813	4363.2	1858.5	434	246.4	77.5	16.1	0
	2.0-2.5	0	0	0	0	0	442	1476	2106.8	559	409.5	46.8	18	0
	2.5-3.0	0	0	0	0	0	0	241.8	1373.7	442.8	98.7	16.4	36.9	3.7
	3.0-3.5	0	0	0	0	0	0	51.1	510.6	214.6	0	83.3	52.8	16.8
	3.5-4.0	0	0	0	0	0	0	0	91.2	353.6	37.2	0	0	0
	4.0-4.5	0	0	0	0	0	0	0	8.7	425.6	105	0	0	0
	4.5-5.0	0	0	0	0	0	0	0	0	163.4	94.9	0	0	0
	5.0-5.5	0	0	0	0	0	0	0	0	0	0	0	0	0

Figure 22. BREF-HB harvestable wave energy matrix

		Tp (s)												
		0-1.0	1.0-2.0	2.0-3.0	3.0-4.0	4.0-5.0	5.0-6.0	6.0-7.0	7.0-8.0	8.0-9.0	9.0-10.0	10.0-11.0	11.0-12.0	12.0-13.0
Hs (m)	0-0.5	0	0	0	0	0	0	0	0	0	0	0	0	0
	0.5-1.0	0	0	0	2334	4257	6327	4475	3510	3432	1550	1166	440	0
	1.0-1.5	0	0	0	1001	15675	37625	36740	16864	8550	5916	1748	546	726
	1.5-2.0	0	0	0	0	4320	31850	121200	64251	21420	15400	4681	854	0
	2.0-2.5	0	0	0	0	0	11645	67240	111752	46410	30765	4589	1560	0
	2.5-3.0	0	0	0	0	0	0	7995	58804	29274	6153	1412	2340	248
	3.0-3.5	0	0	0	0	0	0	1778	21534	15947	0	7208	3768	1140
	3.5-4.0	0	0	0	0	0	0	0	4836	28652	3216	0	0	0
	4.0-4.5	0	0	0	0	0	0	0	574	37968	10620	0	0	0
	4.5-5.0	0	0	0	0	0	0	0	0	15656	10764	0	0	0
	5.0-5.5	0	0	0	0	0	0	0	0	0	0	0	0	0

Figure 23. F2-HB harvestable wave energy matrix

Table 3. Total annual harvestable wave energy for each WEC considered

Wave Energy Converter	Total Annual Harvestable Wave Energy (MWh)
AquaBuoy	287.057
BREF-HB	26.695
F2-HB	960.706

IV. CONCLUSION AND RECOMMENDATIONS

This study created a validated Delft3D-WAVE model that simulated the wave conditions on the sea to the east of Bulusan, Sorsogon for the year 2018. The waves in the study area were found to be wind-generated and comes from the north-north-east direction. During northeast monsoon or Amihan season, waves tend to have an average wave height of around 2 m and period of around 7 s that can grow up to a height of 4 m and period of 10 s. On the other hand, during southwest monsoon season, waves are generally calmer with average height of around 1.25 m and period of 5.5 s. Based on the wave resource matrix, the most frequent wave throughout the entire simulation period has a height of 1.5 to 2 m and corresponding period of 6 to 7 s. The study area is deemed viable as a wave energy resource site as it exceeds the 5 kW/m annual mean power density threshold for feasible WEC installation despite having a moderate-sea state with seasonal variability index of 1.54 and 4 months of low-energy wave conditions. Seasonal deployment and hybridization can be explored to account for this issue

and must be addressed during detailed assessment. Among the 3 WECs considered in this study, F2-HB yielded the highest annual harvestable wave energy at 960.706 MWh, which can supply energy to roughly 1,500 households, or 24% of the residential households in the municipality of Bulusan.

Although it is tempting to conclude that F2-HB is most suitable WEC for the study area, it is important to note that the comparison of the performance of each WEC represents only a preliminary estimate of potential energy yield rather than a definitive device selection. A more compelling conclusion can be achieved regarding the most appropriate WEC if a cost-benefit analysis is conducted, which takes into account operations and maintenance, the capacity factor of each WEC, and performance during extreme conditions. In addition, other types of WEC can be considered for assessment provided they have a published power matrix. Multi-year simulation is also recommended to further assess the interannual variability, e.g. El Niño–Southern Oscillation (ENSO), at the study site. Overall, the methodology conducted in this research provides a template for future researchers or industries that are interested in wave energy harnessing. It can be replicated using secondary data at any location within the country with resolution that is sufficient for preliminary assessment and WEC suitability analysis.

NOMENCLATURE

AWS	Archimedes WaveSwing
BREF-HB	Bottom-Referenced Heaving Buoy
ECMWF	European Centre for Medium-Range Weather Forecasts
ENSO	El Niño–Southern Oscillation
ERA5	Earth Reanalysis 5th generation
F2-HB	Floating 2-Body Heaving Buoy
GEBCO	General Bathymetric Chart of the Oceans
IHO	International Hydrographic Organization
IOC	Intergovernmental Oceanographic Commission
JONSWAP	Joint North Sea Wave Project
MIKE 21 SW	MIKE 21 Spectral Wave model
NAMRIA	National Mapping and Resource Information Authority
NOAA	National Oceanic and Atmospheric Administration
NREP	National Renewable Energy Program
PAGASA	Philippine Atmospheric, Geophysical and Astronomical Services Administration
RMSE	Root-mean-square error
SI	Scatter Index
SSG	Sea Slot-cone Generator
SV	Seasonal Variability
SWAN	Simulating Waves Nearhore
UNESCO	United Nations Educational, Scientific and Cultural Organization
UTC	Coordinated Universal Time
WEC	Wave Energy Converter
WW3	WaveWatch III

References:

[1] Department of Energy. 2023. Retrieved from https://legacy.doe.gov.ph/sites/default/files/pdf/renewable_energy/final_re%20act%20implementation%20status%20report_19%20april%202023.pdf

[2] Philippine News Agency. 2021. Retrieved from https://www.pna.gov.ph/articles/1159659

[3] Quitoras MR, Abundo MLS, Danao LA. 2018. A techno-economic assessment of wave energy resources in the Philippines. Renew. Sustain. Energy. 88:68-81. https://doi.org/ 10.1016/j.rser.2018.02.016

[4] Palconit EV, Villanueva JR, Enano NJ, Buhali MJ, Mascariñas AC, Galope GE, Tabanguil JM. 2021. Resource assessment of tidal stream power in Pakiputan Strait, Davao Gulf, Philippines. Engineering, Technology & Applied Science Research, 11(3), 7233–7239. https://doi.org/10.48084/etasr.3853

[5] Caquilala ER, Abuan BE, Danao LAM. 2023. Techno-economic analysis of tidal energy devices within the Dinagat Islands in the Philippines. Chemical Engineering Transactions. 103:295-300. https://doi.org/10.3303/CET23103050

[6] Villalba IBO, Cleofe EJV, Bautista, DM. 2021. Numerical simulation of tides for the assessment of tidal in-stream energy in selected sites in the Philippines. 3rd International Conference on Smart City Innovation; Bali, Indonesia. IOP Conference Series: Earth and Environmental Science, 673, 012017. https://dx.doi.org/10.1088/1755-1315/673/1/012017

[7] Uehara H, Dilao CO, Nakaoka T. 1988. Conceptual design of ocean thermal energy conversion (OTEC) power plants in the Philippines. Solar Energy. 41(5): 431–441. https://doi.org/10.1016/0038-092X(88)90017-5

[8] Galano RMC, De Leon MP. 2024. Preliminary assessment of potential ocean wave energy resources in the coastal areas of the Philippines. Journal of Coastal Research. 113(sp1):665-669. https://doi.org/10.2112/JCR-SI113-131.1

[9] Wang Z, Jiang D, Dong S et al. 2023. Wave energy resource availability assessment in the Philippines based on 30-Year hindcast data. J. Ocean Univ. China 22:349–364. https://doi.org/10.1007/s11802-023-5044-4

[10] Decapia RJ, Belmonte ZJ, Decapia N, Canta L, Beler PMA. 2025. Assessment of ocean wave energy site mapping in the Philippines: a satellite altimetry and SWAN modeling approach. 5th International Conference on Electrical, Control and Instrumentation Engineering (ICECIE 2024). Lecture Notes in Electrical Engineering. Springer, Cham. https://doi.org/10.1007/978-3-031-83203-1_3

[11] Booij N, Ris RC, Holthuijsen LH. 1999. A third-generation wave model for coastal regions, Part I, Model description and validation. Journal of Geophysical Research: Oceans. 104(C4):7649–7666.

[12] Pacaldo JC, Bilgera PHT, Abundo MLS. 2022. Nearshore wave energy resource assessment for off-grid islands: a case Study in Cuyo Island, Palawan, Philippines. Energies. 15:8637. https://doi.org/10.3390/en15228637

[13] Aminudin A, Teh HM, Pacaldo J. 2021.Wave energy assessment in Dumaran Island, Palawan, Philippines. Int. J. Coast. Offshore Eng. 6:51–63.

[14] GEBCO Compilation Group. 2024. GEBCO 2024 Grid [Data set]. https://doi.org/10.5285/1c44ce99-0a0d-5f4f-e063-7086abc0ea0f

[15] Hersbach H, Bell B, Berrisford P, et al. 2020. The ERA5 global reanalysis. Q J R Meteorol Soc. 146: 1999–2049. DOI: https://doi.org/10.1002/qj.3803

[16] National Centers for Environmental Prediction. 2012. Output fields from the NOAA WAVEWATCH III wave model monthly hindcasts [Data set]. NOAA National Centers for Environmental Information. https://doi.org/10.26023/B0MM-S04D-3Y0Q

[17] Rijkswaterstaat Water . 2015. Retrieved from: https://open.rijkswaterstaat.nl/@125758/comparison-stationary-vs-non-stationary/.

[18] Beya J, Buckham B, Robertson B. 2021. Impact of tidal currents and model fidelity on wave energy resource assessments. Renewable Energy. 176:50–66. https://doi.org/10.1016/ j.renene.2021.05.039

[19] Guillou N, Lavidas G, Chapalain G. 2020. Wave Energy Resource Assessment for Exploitation—A Review. J. Mar. Sci. Eng 8(9):705. https://doi.org/10.3390/jmse8090705

[20] Wu J. 1982. Wind-stress coefficients over sea surface from breeze to hurricane. Journal of Geophysical Research: Oceans. 87(C12):9704–9706. https://doi.org/10.1029/ JC087iC12p09704

[21] Lei Z, Wu W, Gu Y, Zhai F. 2023. A general method to determine the optimal whitecapping dissipation coefficient in the SWAN model. Frontiers in Marine Science. 10:1298727. https://doi.org/10.3389/fmars.2023.1298727

[22] Komen G, Cavaleri L, Donelan M, Hasselmann K, Hasselmann S, Janssen P. 1994. Dynamics and modelling of ocean waves. Cambridge University Press.

[23] Williams JJ, Esteves LS. 2017. Guidance on setup, calibration, and validation of hydrodynamic, wave, and sediment models for shelf seas and estuaries. Advances in Civil Engineering. 5251902: 25.
[24] Mørk G, Barstow S, Kabuth A, Pontes MT. 2010. Assessing the global wave energy potential. ASME 2010 29th International Conference on Ocean, Offshore and Arctic Engineering. p. 447–454. https://doi.org/10.1115/OMAE2010-20473
[25] Cornett AM. 2008. A global wave energy resource assessment. Eighteenth International Offshore and Polar Engineering Conference. p. 318–326.
[26] Carballo R, Arean N, Álvarez M, López I, Castro A, López M, Iglesias G. 2019. Wave farm planning through high-resolution resource and performance characterization. Renewable Energy. p. 1097–1107. https://doi.org/10.1016/j.renene.2018.12.081
[27] Babarit A, Hals J, Muliawan MJ, Kurniawan A, Moan T, Krokstad J. 2012. Numerical benchmarking study of a selection of wave energy converters. Renewable Energy. p. 44–63. https://doi.org/10.1016/j.renene.2011.10.002
[28] Bingölbali B, Çağlar B, Akpınar A, Matrawy KK. 2020. Wave energy resource assessment of the Black Sea. Renewable Energy. 155:1111–1128. https://doi.org/10.1016/ j.renene.2020.04.019
[29] Wilson J, Harper SD. 2022. Wave energy in season: A comparative approach to feasibility of seasonal deployments for remote coastal communities. Energy Reports. 8:10839–10851. https://doi.org/10.1016/j.apenergy.2025.126206
[30] Rasool S, Muttaqi K, Sutanto D. 2020. Assessment of available ocean energy resources and the selection of the conversion technology for a hybrid wind-wave farm in a coastal site of Australia. 2020 IEEE Industry Applications Society Annual Mtg. p. 1-6. https://doi.org/10.1109/IAS44978.2020.9449616.
[31] Sorsogon I Electric Cooperative Inc. (2025). Retrieved from http://www.soreco1.com.